



Partitioning inorganic carbon fluxes from paired O₂–CO₂ gas measurements in a Neotropical headwater stream, Costa Rica

Nicholas S. Marzolf · Gaston E. Small · Diana Oviedo-Vargas · Carissa N. Ganong · John H. Duff · Alonso Ramírez · Catherine M. Pringle · David P. Genereux · Marcelo Ardón

Received: 19 August 2021 / Accepted: 29 June 2022
© The Author(s), under exclusive licence to Springer Nature Switzerland AG 2022

Abstract The role of streams and rivers in the global carbon (C) cycle remains unconstrained, especially in headwater streams where CO₂ evasion (F_{CO_2}) to the atmosphere is high. Stream C cycling is understudied in the tropics compared to temperate streams, and tropical streams may have among the highest F_{CO_2} due to higher temperatures, continuous organic matter inputs, and high respiration rates both in-stream and in surrounding soils. In this paper, we present paired in-stream O₂ and CO₂ sensor data from a headwater stream in a lowland rainforest in Costa Rica to explore temporal variability in

gas concentrations and ecosystem processes. Further, we estimate groundwater CO₂ inputs (GW_{CO₂}) from riparian well CO₂ measurements. Paired O₂–CO₂ data reveal stream CO₂ supersaturation driven by groundwater CO₂ inputs and large in-stream production of CO₂. At short time scales, CO₂ was diluted during storm events, but increased at longer seasonal scales. Areal fluxes in our study reach show that F_{CO_2} is supported by greater in-stream metabolism compared to GW_{CO₂}. Our results underscore the importance of tropical headwater streams as large contributors of carbon dioxide to the atmosphere and show evaded C can be derived from both in-stream and terrestrial sources.

Responsible Editor: Adam Langley

Supplementary Information The online version contains supplementary material available at <https://doi.org/10.1007/s10533-022-00954-4>.

N. S. Marzolf · M. Ardón
Department of Forestry and Environmental Resources,
North Carolina State University, Raleigh, NC, USA
e-mail: nmarzol@alumni.ncsu.edu

G. E. Small
College of Arts and Sciences, University of St. Thomas,
St. Paul, MN, USA

D. Oviedo-Vargas
Stroud Water Research Center, Avondale, PA, USA

C. N. Ganong
Department of Biology, Missouri Western State
University, St. Joseph, MT, USA

J. H. Duff
US Geological Survey, Menlo Park, CA, USA

A. Ramírez
Department of Applied Ecology, North Carolina State
University, Raleigh, NC, USA

C. M. Pringle
Odum School of Ecology, University of Georgia, Athens,
GA, USA

D. P. Genereux
Marine, Earth, and Atmospheric Sciences, North Carolina
State University, Raleigh, NC, USA

Keywords Tropical streams · Carbon cycling · Inorganic carbon · CO_2 evasion · Net ecosystem production

Introduction

Inland waters play an important role in the global carbon (C) cycle and estimates of C fluxes between inland waters, the atmosphere, and terrestrial ecosystems are being revised at a rapid rate (Cole et al. 2007; Raymond et al. 2013; Tank et al. 2018; Drake et al. 2018; Gómez-Gener et al. 2021). Streams, wetlands, and lakes transform, export, and store terrestrial C prior to either delivery downstream to the ocean (Cole et al. 2007) or evasion of CO_2 to the atmosphere (Battin et al. 2009). These processes are particularly important in headwaters streams, which comprise 79% of stream network length (Colvin et al. 2019) and disproportionately contribute to evasion of CO_2 to the atmosphere on an areal basis (Raymond et al. 2013; Borges et al. 2019). However, these findings represent the synthesis from predominantly temperate ecosystems, whereas tropical streams have received less study (Aufdenkampe et al. 2011; Oviedo-Vargas et al. 2015). As a result of higher year-round temperatures, high and continuous organic matter inputs, and drainage from soils with high respiration rates, tropical streams can be hotspots of CO_2 evasion (Borges et al. 2019). In-stream production of CO_2 from mineralization of organic matter can further contribute to high CO_2 fluxes (Richey et al. 2002; Mayorga et al. 2005; Hotchkiss et al. 2015).

Streams are generally CO_2 supersaturated with respect to atmosphere (Wetzel and Likens 2000), reflecting large input fluxes of CO_2 of both terrestrially derived and internally produced CO_2 . Terrestrially derived CO_2 originates from soil respiration and CO_2 -rich geologic formations, which is then transported to headwaters via overland, subsurface, and groundwater flows. In contrast, CO_2 from internal processes is largely the result of respiration of organic matter to CO_2 , though other processes, including photooxidation (Rocher-Ros et al. 2021) and CH_4 oxidation (Lupon et al. 2019), contribute to total internal production. In headwater streams, the influence of terrestrially derived CO_2 is predicted to be greater than internal production and to decrease in magnitude in larger streams and rivers (Hotchkiss et al. 2015).

Losses of CO_2 from streams include evasion to the atmosphere, uptake through photosynthesis, and hydrologic export downstream. Evasion of CO_2 from freshwaters is a large flux of C largely unaccounted for in terrestrial budgets (Genereux et al. 2013) and is important at global scales (Raymond et al. 2013; Liu et al. 2022). Hydrologic export of dissolved inorganic carbon (DIC) comprises aqueous CO_2 , H_2CO_3 , HCO_3^- , and CO_3^{2-} , which speciate according to pH (Stumm and Morgan 1996). High concentrations of CO_2 may reduce pH by an amount that depends on the buffering capacity of the water (Wetzel and Likens 2000; Small et al. 2012) and accelerate dissolution of carbonate minerals (Stoddard et al. 1999).

Advances in sensor technology allow measurement of CO_2 and O_2 at high frequency in freshwaters (Johnson et al. 2010), permitting estimation of fluxes of these gases under different hydrologic conditions (e.g., base or storm flows) and as drivers of stream physicochemistry. Results from discrete sampling of F_{CO_2} have revealed important aspects of underlying ecological and morphological processes, including the importance of gas exchange rates and depth (Rasera et al. 2013; Campeau et al. 2014; Oviedo-Vargas et al. 2015). Aquatic sensors allow differentiating C sources and sinks at higher frequency and under conditions hard to capture using discrete sampling (e.g., floods). Further, coupling net ecosystem productivity (NEP) estimates with CO_2 sensor data allows for finer accounting of CO_2 , variability during base and storm flow events, and evaluation of processes that affect concentrations of both gases together (e.g., gas exchange, respiration) and separately (e.g., anaerobic respiration) (Vachon et al. 2020; Aho et al. 2021b; Haque et al. 2022). The advance in CO_2 sensing demonstrates that temporal variation at short (e.g., storm event) and longer (e.g., growing season) scales across the continental US is multi-faceted, driven by interactions among stream biology, physics, and hydrology (Crawford et al. 2017). While combining CO_2 and O_2 sensor data in headwater streams to partition and account for various sources and sinks has been applied in Arctic and temperate streams (Lupon et al. 2019; Rocher-Ros et al. 2020), these methods have not been applied in tropical streams.

In this paper, we present the results of continuous deployment of in-stream and riparian well sensors to estimate areal and volumetric C fluxes in

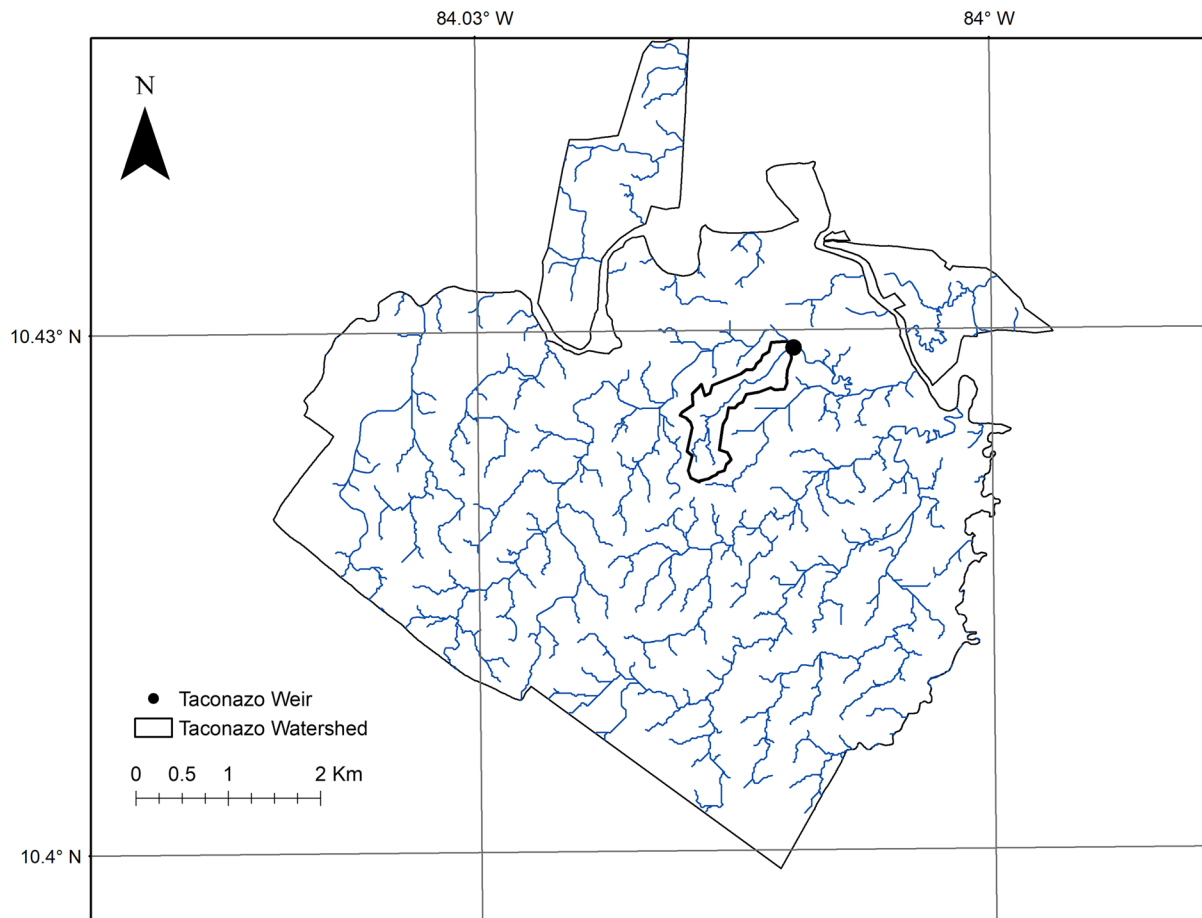


Fig. 1 Map of La Selva Biological Station, Costa Rica, with the Taconazo watershed outlined in black. The weir near the outflow is designated at the black circle. Blue lines are the

stream network. Figure S1 has additional details on the sensor deployment and reach delineation

a headwater Neotropical stream, Costa Rica. We simultaneously estimate reach CO_2 losses as evasion (F_{CO_2}), and CO_2 inputs as NEP and terrestrial CO_2 from groundwater (GW_{CO_2}) at hourly intervals for six months, allowing comparison of fluxes at short- (event) and long-term (seasonal) hydrologic conditions. We hypothesized that: (1) O_2 would be undersaturated and CO_2 would be supersaturated relative to the atmosphere due to in-stream respiration, (2) $p\text{CO}_2$ would decrease at short time scales due to dilution (e.g., storm events) and increase at long-term scales from sustained terrestrial inputs (e.g., seasonal), (3) external fluxes of CO_2 would exceed internal CO_2 production following the theoretical predictions for low order streams (Hotchkiss et al. 2015), and (4) stream pH would decrease

with elevated GW_{CO_2} as predicted by carbonate equilibrium.

Methods

Site description

Our study took place at La Selva Biological Station, Costa Rica (LSBS), a 1600 ha tropical wet forest reserve, with elevation ranging from 22 to 146 m above sea level (Fig. 1). LSBS is located at the transition from the upland foothills of the Cordillera Central of Costa Rica and the Caribbean lowlands, and is the lowland terminus of the altitudinal transect in the Braulio Carrillo National Park (Fig. 1). Mean annual

Table 1 Reach characteristics from Taconazo and summary statistics for physicochemical data during the study period

Measurement (unit)	Value
Reach length (m)	75
Mean reach width (m) ^a	1.3
Mean reach velocity (m s ⁻¹) ^a	0.014
Travel time (min) ^a	82.5
Gradient (m m ⁻¹)	0.0024
Temperature (°C)	24.5 (21.2–29.6)
DO (mg L ⁻¹)	5.94 (0.26–8.32)
pH	5.32 (4.02–6.91)
pCO ₂ (ppmv)	6443.6 (773.8–11,994)
Stream discharge (m ³ s ⁻¹) ^b	0.017 (0–1.378)

High frequency data (temperature, DO, pH, pCO_2 , and stream discharge) are presented as the median (range in parentheses) during the monitoring period

^aMeasured in March 2013

^bExcludes backflooding events when the downstream Rio Puerto Viejo floods its tributaries, including Taconazo (Zanon et al. 2014)

rainfall is 4300 mm, with a dry season from January to April and a wet season from May to December (Sanford et al. 1994).

We focused our study in a 75 m reach of the Taconazo stream (10.432°N, 84.013°W) to quantify and partition CO₂ fluxes. The Taconazo watershed area is 0.270 km², all of which is forested with a closed canopy (Table 1). Taconazo is a low solute stream at LSBS, with long-term (1997–2015) mean water temperature of 25.1 °C, pH of 5.5, discharge of 0.06 m³ s⁻¹, and NO₃⁻ and soluble reactive phosphorus concentrations of 192.4 µg L⁻¹ and 4.9 µg L⁻¹, respectively (Ganong et al. 2015). Taconazo has received significant study as a model headwater lowland tropical stream. Numerous studies from Taconazo have investigated its hydrology (Genereux et al. 2005, 2009; Genereux and Jordan 2006; Solomon et al. 2010), biogeochemistry (Small et al. 2012; Oviedo-Vargas et al. 2015; Osburn et al. 2018), and ecology (Ardón et al. 2006; Ramírez et al. 2003; Rosemond et al. 2002).

Data collection

We collected stream data from April 1, 2013 to September 30, 2013. Discharge (Q, m³ s⁻¹) was continuously measured at a sharp-crested 90-degree

V-notch weir constructed near the downstream end of Taconazo (Genereux et al. 2005). Rainfall (mm) was collected from the LSBS weather station, located ~ 900 m from Taconazo. Meteorological data are available at <https://tropicalstudies.org/>.

We secured a YSI 600xlm multiprobe sonde 5 cm above the stream bottom at the downstream end of the study reach and just upstream of the pool created at the weir (Fig. S1). The sonde was placed in a PVC tube with holes drilled to allow for exchange of stream water and secured to a rebar stake in the stream bed. The sonde continuously measured temperature (°C), pH, and DO (mg L⁻¹ and %-saturation) at hourly intervals. The sonde was retrieved every 2 weeks for recalibration and to clean fouling on the sensor heads. Partial pressure of CO₂ (ppmv) was measured using a Vaisala GMT221 infrared gas analyzer (IRGA) in the stream and in a riparian well. The sensors were prepared for submerged deployment as described in Johnson et al. (2010) and pCO_2 was logged hourly using a Campbell CR1000 datalogger. As pCO_2 was measured under water, the data were corrected for depth and temperature (Johnson et al. 2010). We excluded data from all sensors when the water level fell below the height of the sonde (e.g., conductivity < 0.005, DO near air saturation), which was 8.5% (~ 15 days) of the dataset. Sensor data underwent further QAQC following the guidance of Taylor and Loescher (2013) and visual examination using the datacleanr R package v 1.0.3 (Hurley 2021). The sensor schematic and deployment stations in the stream are shown in Fig. S1.

To evaluate the precision of the sensor, we compared the estimates of CO₂ from the in-stream sensor to headspace samples. Headspace samples were collected weekly from Taconazo by collecting 4 mL of stream water into a 10 mL syringe and injecting the sample into an inverted sealed serum vial pre-filled with 100 µL of HCl with a 22-gauge needle and a 0.45 µm pore filter. Samples were equilibrated on a shaker table, after which a 250 µL headspace was removed and pCO_2 analyzed on an SRI Instruments gas chromatograph (Las Vegas, Nevada, USA) equipped with a thermal conductivity detector and 3-foot silica gel column (He carrier flow rate 10 mL min⁻¹, detector 150 °C, oven 90 °C). For both sensor and headspace measurements of pCO_2 , we calculated [CO₂]_{aq} using temperature-dependent Henry's Law constant (Plummer and Busenberg 1982) and

calculated $[\text{CO}_2]_{\text{sat}}$ assuming an atmospheric concentration of 400 ppmv CO_2 (Rocher-Ros et al. 2020). To ensure all dissolved inorganic C (DIC) was captured, we converted $[\text{CO}_2]_{\text{aq}}$ to DIC by calculating ionization fractions (Appendix 1 Eqs. 4–6, 8). Sensor and headspace measures of DIC were compared using a Student's *t* test.

Evaluating aqueous concentrations of CO_2 and O_2

For each hourly measurement of O_2 and CO_2 , we calculated the respective saturation concentration, assuming the aqueous gas was in equilibrium with the atmosphere. For O_2 , concentration at saturation ($\text{O}_{2-\text{sat}}$) was calculated as a function of barometric pressure and temperature (see functions in Hall and Hotchkiss 2017). For CO_2 , we calculated aqueous CO_2 from both measured in-stream ($[\text{CO}_2]_{\text{aq-str}}$) and in the riparian well ($[\text{CO}_2]_{\text{aq-well}}$) using a temperature dependent Henry's Law constant (Plummer and Busenberg 1982) and calculated $[\text{CO}_2]_{\text{sat}}$ assuming an atmospheric concentration of 400 ppmv CO_2 (Rocher-Ros et al. 2020).

For both measured and saturation concentrations of the in-stream gases, we measured departure, $\text{CO}_{2-\text{dep}}$ and $\text{O}_{2-\text{dep}}$, as the difference of measured concentration from saturation concentration. Departure concentrations were plotted as a data cloud for each month, $\text{O}_{2-\text{dep}}$ vs. $\text{CO}_{2-\text{dep}}$. For each month, we calculated the: (1) location of the cloud centroid, and (2) 1/slope the inverse of the slope of a best-fit line through each month's data cloud. The inverse slope shows the efficiency of metabolism, interpreted as the moles of CO_2 produced per moles of O_2 consumed during ecosystem respiration.

Response of CO_2 to storm events

To evaluate the role of storms on $p\text{CO}_2$ during the monitoring period, we compared gas concentrations during high and low flow events. We used a hydrograph separation approach to determine baseflows and storm flow discharges for each hour in our time series. We used a modified Lyne–Hollick filter, which uses a recursive data filtering approach to separate baseflow for a given hydrograph (Ladson et al. 2013). The approach relies on a filter parameter, α , to determine the volume of baseflow and volume of storm flow. We assessed a range of α values from 0.9 to 0.99

for Taconazo (Fig. S2) and visually determined α of 0.96. The separation filter identified each discharge measurement as baseflow when the fraction of baseflow ≥ 0.5 or stormflow when the fraction < 0.5 .

To evaluate $p\text{CO}_2$ during storm and baseflow conditions, we compared $p\text{CO}_2$ in each month and in each flow condition. We used a non-parametric two-way Aligned Rank Transform (ART) test to determine which months and flow conditions had greater $p\text{CO}_2$. Hydrograph separation was calculated in the hydrostats R package v 0.2.8 using the baseflows() function (Bond 2021) and ART in the ARTool v 0.11.1 R package (Kay and Wobbrock 2020).

Reach-scale CO_2 fluxes

The sensor deployment in the stream and riparian well allowed us to calculate reach-scale areal fluxes within the focal reach. We simultaneously estimated CO_2 inputs through groundwater (GW_{CO_2}) and net ecosystem production (NEP), and outputs as evasion to the atmosphere (F_{CO_2}).

Estimates of GW_{CO_2} were calculated as the product of groundwater discharge into the study reach and $[\text{CO}_2]$ measured in the well. Groundwater discharge into the lower Taconazo reach had been determined using both instantaneous and continuous conservative tracer injections to the stream (Ardón et al. 2013; Oviedo-Vargas et al. 2015). In a 132 m reach, groundwater discharge was measured as 17.8% (dry season) and 7.2% (wet season) of stream discharge (Oviedo-Vargas et al. 2015). In the same 75 m reach in this study during the dry season, groundwater discharge was 9% of stream discharge (Ardón et al. 2013). We favor this approach, which uses empirical field data, to alternatives (e.g., hydrograph separation, see above), which introduce uncertainty (Fig. S2, S5–S11) into our process-based flux estimates.

We estimated groundwater discharge (Q_{GW}) into the 75 m study reach upstream of the weir every hour as

$$Q_{\text{GW}} = f_{\text{GW}} * Q \quad (1)$$

where f_{GW} is the percent change in stream discharge from conservative tracer injections, equal to 17.8% for the dry season (April) and 7.2% for the wet season (May–September), and Q is total hourly discharge ($\text{m}^3 \text{ h}^{-1}$). The seasonal approximation of Q_{GW} as a

fraction of Q assumes no temporal variation in f_{GW} into the reach. The lack of variation is unlikely given the seasonality of rainfall, but the data to determine the variability could not be collected to the same accuracy as the other parameters and the percentages used reflect discrete sampling with high accuracy (Genereux et al. 2005; Ardón et al. 2013; Oviedo-Vargas et al. 2015).

Groundwater CO₂ flux (mol CO₂ m⁻² h⁻¹) was calculated as input of CO₂ in groundwater that enters the stream bed area in the study reach

$$GW_{CO_2} = [CO_2]_{aq-well} * \frac{Q_{GW}}{L*w} \quad (2)$$

where L is the length of the reach (75 m), w is the wetted width (1.5 m in the dry season and 2.8 m in the wet season), and Q_{GW} (m³ h⁻¹) is estimated from Eq. 1.

Areal CO₂ inputs were also quantified through NEP, or the net internal production of CO₂ through aerobic processes. We estimated NEP as

$$NEP_i = \left(\frac{O_i - O_{i-\Delta t}}{\Delta t} - K_{O2}(O_{sat,i} - O_i) \right) * \bar{z} \quad (3)$$

where NEP_i is hourly instantaneous metabolism (mol O₂ m⁻² h⁻¹), O_i is the O₂ concentration in the stream at each timepoint, i (mol m⁻³), O_{i-Δt} is O₂ at the preceding timepoint, O_{sat,i} is the concentration of O₂ at saturation for the same timepoint (mol m⁻³), \bar{z} is mean reach depth (m), and K_{O2} is the gas exchange coefficient for O₂ (h⁻¹). We used values of K_{O2} measured from dry (19.5 d⁻¹) and wet (7.3 d⁻¹) season tracer gas injections of propane (Oviedo-Vargas et al. 2015), converted in terms of O₂ using Schmidt scaling; see Appendix 2 for calculations. NEP was converted to mol C m⁻² h⁻¹ assuming a 1:1 respiratory quotient between O₂ and CO₂ (Rocher-Ros et al. 2020). We selected the direct metabolism method for determining NEP because the lack of a diel O₂ signal (Fig. S3) and relatively high reaeration make Taconazo ill-suited to alternative stream metabolism methods (Appling et al. 2018; Hall and Ulseth 2020). Further, the direct method allows for estimation of NEP at finer temporal compared to alternative approaches, which are resolved at the daily scale.

Reach-scale losses of CO₂ were estimated as evasion to the atmosphere. F_{CO2} was estimated as:

$$F_{CO_2} = ([CO_2]_{aq-str} - [CO_2]_{sat}) * K_{CO_2} * \bar{z} \quad (4)$$

where [CO₂]_{aq-str} and [CO₂]_{sat} (mol m⁻³) are concentrations described in the above text, K_{CO2} is the gas exchange coefficient for CO₂ (h⁻¹) and \bar{z} is mean reach depth (m). As with K_{O2} above, we used seasonal measurements of dry (20.3 d⁻¹) and wet (7.6 d⁻¹) season gas exchange from propane injections and converted to K_{CO2} using Schmidt scaling (Raymond et al. 2012).

Reach-scale fluxes were aggregated to daily time steps by summing hourly fluxes. Negative values of NEP (mol C m⁻² d⁻¹) indicate net daily consumption of CO₂, likely through photosynthesis, whereas positive NEP indicate net production of CO₂ through aerobic respiration. Daily areal inputs (GW_{CO2} and NEP) were evaluated as drivers of outputs (F_{CO2}) using linear regression. Finally, we evaluated the influence of daily GW_{CO2} on mean daily pH, hypothesizing greater GW_{CO2} would decrease pH. We regressed log₁₀ GW_{CO2} against mean daily pH, removing 4 days of mean daily pH outliers (pH < 4.8 and pH > 5.9). All calculations and statistics were completed in R v 4.1.2 (R Core Team 2022) and are available in Appendix 2.

Results

Stream data

Total rainfall during the 180-day monitoring period was 2067 mm, with median daily rain of 2.29 mm (range: 0–107 mm) and 49 days with no rainfall recorded (Fig. 2a). April had the lowest rainfall (104.1 mm) and June had the most rainfall (498.6 mm). Median hourly stream discharge was 0.004 m³ s⁻¹ (0–1.378 m³ s⁻¹ range). Median discharge was lowest in April (0.0002 m³ s⁻¹) and greatest in July (0.0160 m³ s⁻¹). Median estimated groundwater flux into the reach was 0.0003 m³ s⁻¹ (0–0.0346 m³ s⁻¹ range) (Fig. 2b). Median pCO₂ in the stream was 6343.6 ppmv (range 773–11,994 ppmv), lower than that measured in the riparian well (median pCO₂ 46,924 ppmv, range 28,663–48,683 ppmv). Over the monitoring period, 14% of hourly stream pCO₂ measurements were missed, the largest missing section corresponding with the highest flows in late July

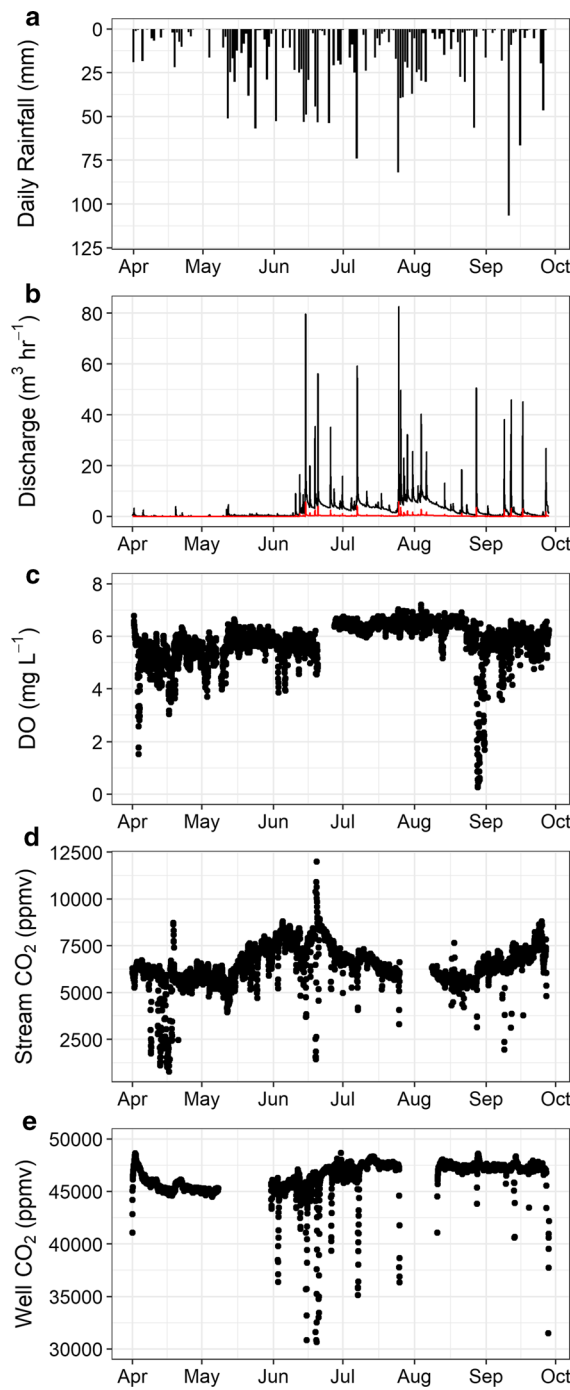


Fig. 2 **a** Daily rainfall, **b** total hourly stream (black line) and groundwater (red line) discharge ($\text{m}^3 \text{h}^{-1}$) in Taconazo, and hourly **c** dissolved oxygen (mg L^{-1}) in the stream water, **d** stream water $p\text{CO}_2$ (ppmv), and **e** groundwater well $p\text{CO}_2$ (ppmv) in the riparian well

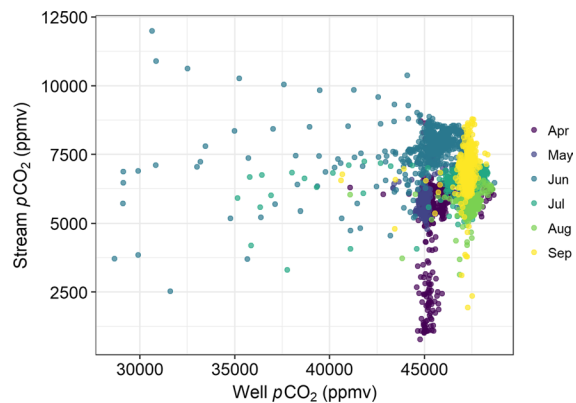


Fig. 3 Measured $p\text{CO}_2$ from the in-stream and riparian well stations in Taconazo. Points are colored by the month of data collection. See Fig. S1 for photos of deployment locations and schematics

and early August (Fig. 2d). In the riparian well, 27% of hourly measurements were missing, including the same period missing from the stream time-series and a period in May, during the transition from dry to wet season (Fig. 2e). There was no pattern between stream $p\text{CO}_2$ and well $p\text{CO}_2$, reflecting the sustained high well $p\text{CO}_2$ (Fig. 3). Estimates of DIC from both discrete sampling (mean $0.23 \pm 0.06 \text{ mmol DIC L}^{-1}$) and from the sensor (mean $= 0.25 \pm 0.04 \text{ mmol DIC L}^{-1}$) were similar ($p=0.34$).

Evaluating aqueous concentrations of CO_2 and O_2

In comparing O_2 and $p\text{CO}_2$ to their atmospheric saturation, most timepoints showed CO_2 supersaturation and O_2 undersaturation (Fig. 4). CO_2 departure was ~ 6.6 -times greater than O_2 departure, on average. Ellipse centroid location varied little over time (Table 2). The value of $1/\text{slopes}$ was greatest in September (467.9) and lowest in August (0.7). The general position of the cloud away from the 1:1 line and closer to the x-axis indicates aerobic metabolic processes are not responsible for controlling CO_2 and O_2 , and the higher concentration of CO_2 than O_2 suggests CO_2 in excess due to either anaerobic respiration or external inputs (e.g., groundwater).

Response of CO_2 to storm events

Hydrograph separation identified 2930 h of baseflow and 1394 h of storm flow (Fig. 5a). Median

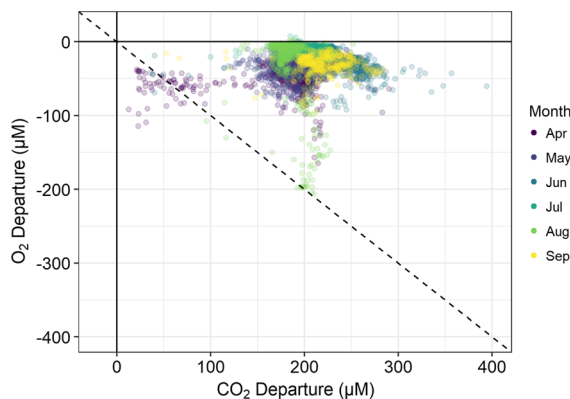


Fig. 4 Paired O₂ and CO₂ departure from atmospheric equilibrium. The color of the points indicate the month collected and richer colors reflect a higher density of points. The dashed line is the 1:-1

Table 2 Paired O₂–CO₂ metrics for each month of the monitoring period

Month	Mean CO ₂ -Dep ± SD (µM)	Mean O ₂ -Dep ± SD (µM)	1/[Slope] (µM µM ⁻¹)
April	175.5 ± 46.6	– 48.6 ± 18.4	20.5
May	190.3 ± 20.7	– 45.7 ± 14.9	6.2
June	245.8 ± 26.5	– 32.0 ± 15.2	5.6
July	207.7 ± 15.4	– 11.1 ± 5.2	13.4
August	183.0 ± 14.9	– 31.5 ± 46.5	0.7
September	221.2 ± 25.2	– 30.6 ± 12.8	467.9
All dates	203.8 ± 38.5	– 32.0 ± 26.5	16.7

Mean CO₂-Dep and O₂-Dep are mean monthly concentrations followed by standard deviation in parentheses. The 1/[slope] is the slope of the linear model fit through each months' data. The paired mean departures are coordinates in Fig. 3 for each month

baseflow increased from $5.5 \times 10^{-7} \text{ m}^3 \text{ s}^{-1}$ in April to $8.8 \times 10^{-4} \text{ m}^3 \text{ s}^{-1}$ in July. June, July, and August had the greatest median baseflow ($\geq 1 \times 10^{-3} \text{ m}^3 \text{ s}^{-1}$), compared to April, May, and September, where median baseflow was $\leq 1 \times 10^{-4} \text{ m}^3 \text{ s}^{-1}$. For all months, mean pCO₂ was greater during baseflow than stormflow by $1146 \pm 44.6 \text{ ppmv}$ ($p < 0.01$; Fig. 5b).

Reach-scale CO₂ fluxes

Reach scale CO₂ fluxes varied over time (Fig. 6a–c). On average, median (\pm sd) GW_{CO₂} ($9.5 \times 10^{-3} \pm 0.03 \text{ mol CO}_2 \text{ m}^{-2} \text{ d}^{-1}$) was less than median NEP

($2.8 \times 10^{-2} \pm 0.16 \text{ mol CO}_2 \text{ m}^{-2} \text{ d}^{-1}$). GW_{CO₂} was lowest in May (median $7.0 \times 10^{-5} \text{ mol CO}_2 \text{ m}^{-2} \text{ d}^{-1}$) and greatest in July ($4.9 \times 10^{-2} \text{ mol CO}_2 \text{ m}^{-2} \text{ d}^{-1}$). NEP was greatest in April (median $0.13 \text{ mol CO}_2 \text{ m}^{-2} \text{ d}^{-1}$), but mean NEP was less than $0.1 \text{ mol CO}_2 \text{ m}^{-2} \text{ d}^{-1}$ for all other months. Evasion similarly varied over time. Median F_{CO₂} was $0.18 \pm 0.14 \text{ mol CO}_2 \text{ m}^{-2} \text{ d}^{-1}$, but was greatest in April (median $0.38 \text{ mol CO}_2 \text{ m}^{-2} \text{ d}^{-1}$) and lowest in September ($0.07 \text{ mol CO}_2 \text{ m}^{-2} \text{ d}^{-1}$). There was no relationship between GW_{CO₂} and F_{CO₂} ($F_{1,133} = 0.02$, $p = 0.88$; Fig. 6d), in contrast to the relationship between NEP and F_{CO₂} ($F_{1,133} = 7.11$, $p < 0.01$; Fig. 6e). Finally, stream pH was negatively correlated with GW_{CO₂} ($F_{1,131} = 33.8$, $p < 0.01$; Fig. 7).

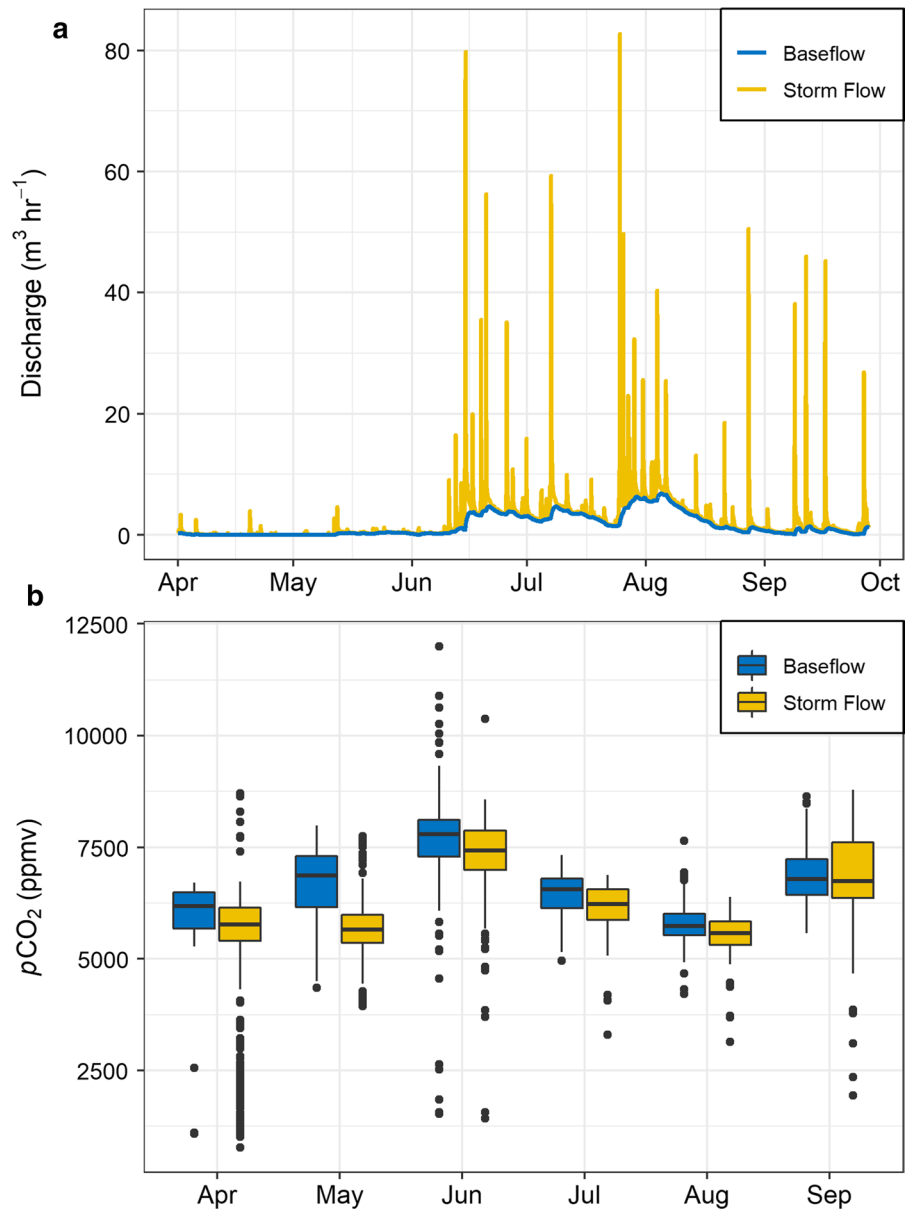
Discussion

In this study, we combined stream and riparian well aquatic gas sensors to quantify temporal variation of pCO₂ and O₂, and CO₂ input and output fluxes in a Neotropical headwater stream. The results show sustained high pCO₂ in the stream relative to the atmosphere, and pCO₂ was greater during baseflow than during storms. Elevated pCO₂ led to high F_{CO₂}, sustained by higher CO₂ inputs from both NEP and GW_{CO₂}, in contrast to theoretical predictions that suggest greater groundwater contributions in headwater streams. Last, GW_{CO₂} contributes to lower pH in the stream and defines a possible mechanism for understanding drivers of episodic and seasonal acidification events (Small et al. 2012; Ganong et al. 2021). Our analysis highlights the use of combined sensor arrays in estimating multiple reach-scale CO₂ fluxes and posits a method to estimate terrestrial CO₂ losses to the hydrologic cycle. We found F_{CO₂} to be a major loss of C from the Taconazo, underscoring the importance of considering fluxes from headwater streams in complete C assessments and budgets.

Evaluating aqueous concentrations of CO₂ and O₂

The monitoring period included one month of the dry season with the remaining five months during the wet season (Sanford et al. 1994). The transition from dry to wet season is reflected by the increased rainfall in mid-May (Fig. 2a). The dry to wet transition coincides with a seasonal increase

Fig. 5 **a** Separated hydrograph, with baseflow (blue line) and storm flow (yellow line), summing to total discharge. **b** $p\text{CO}_2$ measured in each month during each of the flow conditions, baseflow (blue boxplots) or storm flow (yellow boxplots). Boxplots show median, 25th and 75th quartiles, and outliers > 10th and 90th percentiles



in stream $p\text{CO}_2$ (Figs. 2d and 5b), though there was little increase in riparian well $p\text{CO}_2$ (Fig. 3). $p\text{CO}_2$ measured in Taconazo (median $p\text{CO}_2 = 6343$ ppmv) was high relative to similarly sized streams in a monitoring study across headwater streams in North America. Taconazo $p\text{CO}_2$ was higher than 6 of the 7 streams monitored, only less than a site in a southern hardwood forest and greater than a highland tropical stream in Puerto Rico (Crawford et al. 2017). We observed little diel variability in $p\text{CO}_2$ or O_2 (Fig. S2), indicating gross primary productivity

(GPP) is low in Taconazo, and supported by the NEP estimates $> 0 \text{ mol C m}^{-2} \text{ h}^{-1}$ (Fig. 6b).

The paired CO_2 – O_2 cloud (Fig. 4) is located far from the 1:-1 line, with CO_2 in excess of O_2 . This reflects CO_2 supersaturation and O_2 undersaturation, and the deviance from the 1:-1 line indicates aerobic ecosystem processes do not regulate CO_2 and O_2 . In tundra headwater streams, the location of the CO_2 – O_2 departure cloud was closer to the 1:-1 line and reflected the greater influence of in-stream

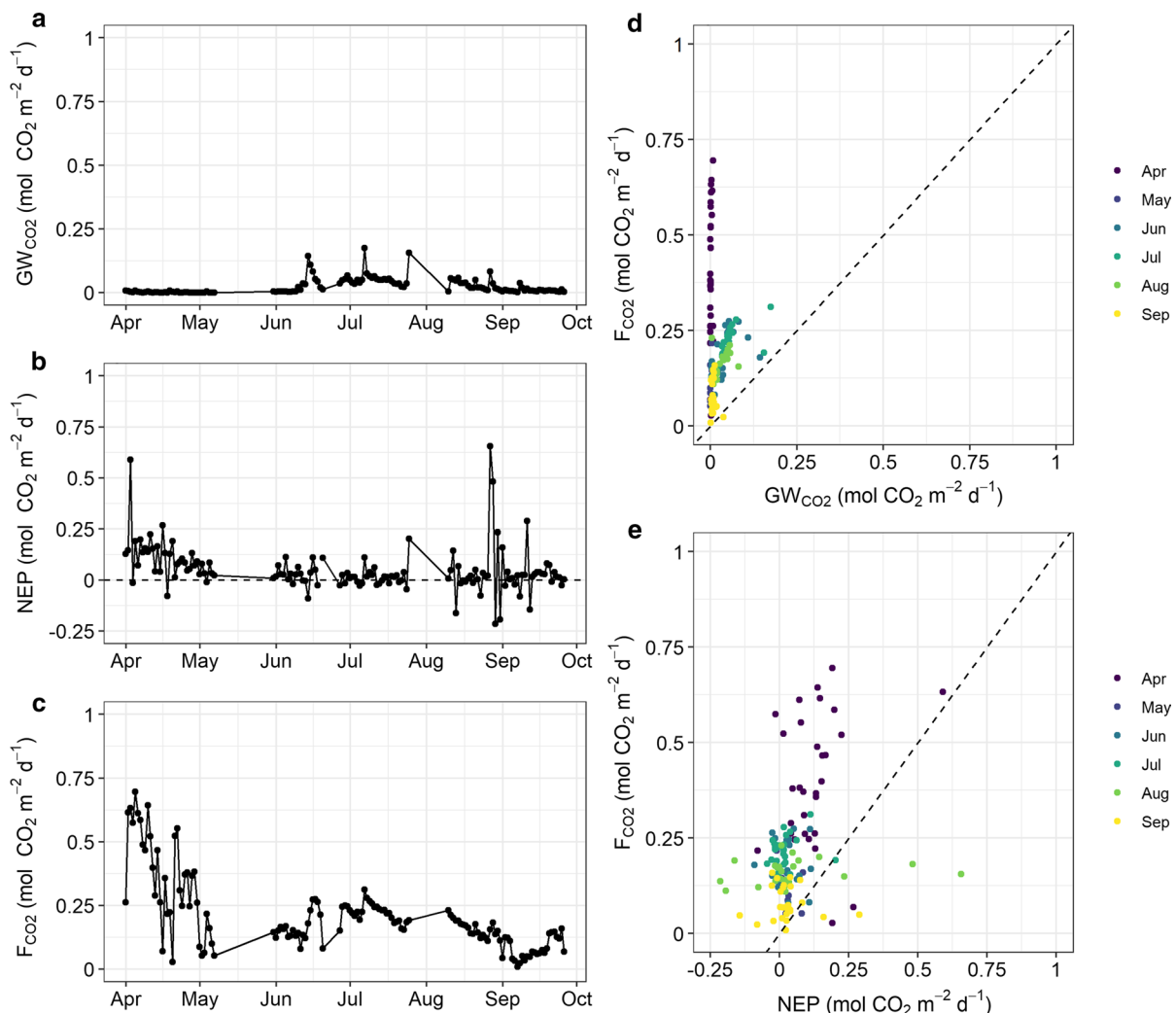


Fig. 6 Areal fluxes measured in the lower Taconazo study reach. Left panels show time series of daily areal fluxes for **a** groundwater CO_2 , **b** net ecosystem production, and **c** evasion. Right panels show the correlation of evasion with each input flux **d** groundwater and **e** net ecosystem production, with

points colored by month of the measurement. Dashed lines in **b** at $NEP=0$, and $NEP>0$ indicates net carbon production and $NEP<0$ indicates net carbon consumption; lines in **d** and **e** are 1:1 lines

NEP on F_{CO_2} (Rocher-Ros et al. 2020). The location of the data cloud away from the 1:-1 line suggests that aerobic metabolism is not a dominant process in Taconazo and is not responsible for simultaneously driving O_2 and pCO_2 . In contrast, anaerobic respiration may be an important contribution of CO_2 to the stream from riparian soils or in-stream sediments, to account for the supersaturation not attributed to aerobic respiration.

Response of CO_2 to storm events

The hydrograph separation shows that storm flows dilute pCO_2 , but increasing pCO_2 occurs at longer, seasonal scales. Dilution during high flows is likely, as median discharge increases by a factor of 7.5 from base ($0.22\text{ m}^3\text{ h}^{-1}$) to storm ($1.62\text{ m}^3\text{ h}^{-1}$) flows. Dilution in CO_2 concentration during storm events indicates pCO_2 of surface flows and shallow subsurface flows are lower than pCO_2 measured in deep soils and in-stream, though total flux during the

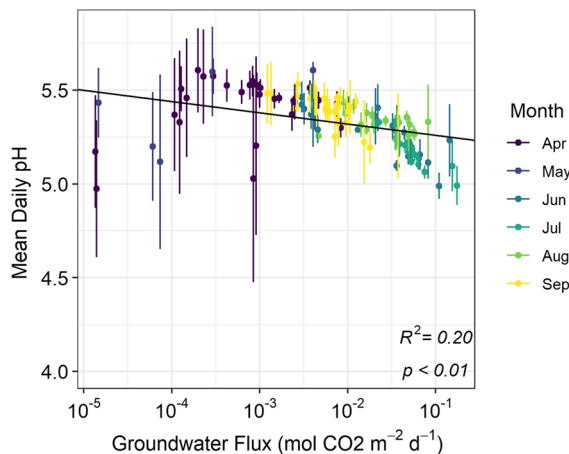


Fig. 7 Groundwater CO₂ flux as a driver of the mean stream pH. Black line is line-of-best fit. Point color indicates the month and vertical bars for each point represent the pH daily standard deviation

different flow conditions may be similar, as has been shown for DOC (Osburn et al. 2018). Additionally, decreased *p*CO₂ during storm flows may result from increased evasion during high flow events as storms can increase turbulence and increase gas exchange during the event (Raymond et al. 2012; Hall and Ulseth 2020), which reduces *p*CO₂ during storm events. Increased *p*CO₂ during baseflow conditions suggest reach scale input fluxes predominate during baseflow periods. While NEP estimates across ranges of discharge are uncommon, elevated *p*CO₂ during baseflows reflect greater mineralization of CO₂ through NEP. Increased dissolved organic C (DOC) fluxes in storm events fueled in-stream respiration in peat streams (Demars 2019), suggesting similar storm flow related pulses of DOC (Osburn et al. 2018) could fuel increased CO₂ mineralization. Seasonal increases in *p*CO₂ from the dry to the wet season reflect the increase in GW_{CO₂} in June and July (Fig. 6a).

Reach-scale CO₂ fluxes

Headwater streams are predicted to receive a greater fraction of C from external sources relative to in-stream production due to contributing drainage area compared to stream-bed area. However, our data show a larger contribution of internally-produced CO₂. For example, models for temperate streams indicate

external inputs of C (i.e. GW_{CO₂}) to be greater than internal production (i.e. NEP) in low-order streams (Hotchkiss et al. 2015). Our results do not entirely support this hypothesis, as GW_{CO₂} was often a lower contributor of CO₂ to the total flux than NEP. In part, this could be to underestimates of GW_{CO₂} that derive from lack of contribuus estimates of f_{GW}. In addition, our methods do not capture shallow subsurface flow and overland flow, which could be contributing to CO₂ inputs in the reach. Estimates of GW_{CO₂} could be improved with greater understanding of the temporal variation of f_{GW}, both between and within the dry and wet seasons and using alternative approaches to minimize uncertainty at the scale of our data collection. Beyond the uncertainty in hydrologic approaches, our deployment of sensors in a riparian well represents a method to estimate C losses to the hydrologic cycle from terrestrial systems. Given the sustained CO₂ measured in the riparian well (Fig. 3), which are similar to soil CO₂ measured in forested headwater streams in the Amazon (Johnson et al. 2008), we highlight the need to understand variation in groundwater inputs, as a large fraction of soil-derived CO₂ is quickly evaded to the atmosphere.

Estimates of NEP reveal aerobic processes were a source of C to the stream and were often larger in magnitude than GW_{CO₂}. Estimates of NEP showed little temporal variation (Fig. 6b) and are derived from undersaturated DO measurements throughout the period (Figs. 2c and 4) and lack diel variation (Fig. S3). The magnitude of NEP was not affected by variability in gas exchange rates (Fig. S4, b), which confirms the consistent undersaturation of O₂ relative to the atmosphere (Fig. 2c). The NEP estimates were similar to streams and rivers in the tropics (median NEP = 0.9 mol C m⁻² d⁻¹, compare to NEP = 1.5 mol C m⁻² d⁻¹ (Marzolf and Ardón 2021)), and NEP was a stronger contributor to F_{CO₂} than GW_{CO₂} (Fig. 6e). In-stream contribution to F_{CO₂} was also shown in tundra streams with higher primary production (Rocher-Ros et al. 2020). In-stream gross primary production is likely low due to light limitation exerted by the forest canopy, resulting in C cycling in the stream driven by allochthonous organic matter.

Evasion estimates were high and of similar magnitude to previous work in Taconazo. We estimate a median F_{CO₂} 0.18 ± 0.14 mol C m⁻² d⁻¹, which are similar to fluxes calculated from headspace samples from the dry (0.9 ± 0.4 mol C m⁻² d⁻¹) and

wet ($0.6 \pm 0.3 \text{ mol C m}^{-2} \text{ d}^{-1}$) season in the same stream (Oviedo-Vargas et al. 2015). Our estimates rely on seasonal gas exchange measurements from Oviedo-Vargas et al. (2015), though the similarity in F_{CO_2} estimates support the sensor measurements of $p\text{CO}_2$. Further, in our study F_{CO_2} is likely underestimated. Our estimates rely on seasonal measurements of gas exchange, and improved understanding of temporal variation and relationship of gas exchange with stream morphology and hydrology in Taconazo would increase the precision of our estimates. Scaling equation estimates of gas exchange that rely on morphologic parameters, like depth, width, and discharge, are ill-suited to process based C estimates (Raymond et al. 2012). Inverse models rely on sufficient GPP to estimate gas exchange from a diel O_2 curve (Hall and Ulseth 2020), which are absent in our data (Fig. S3). Last, we highlight the sensitivity of F_{CO_2} to variation in gas exchange (Fig. S4), which indicate transport limitation, or F_{CO_2} controlled by flow and morphologic characteristics rather than C supply (Schneider et al. 2020).

For many headwater streams, F_{CO_2} is the dominant fate of aqueous CO_2 , but comparing this flux to other CO_2 losses is an important consideration to understand the stream C cycle. We compared F_{CO_2} from Taconazo to hydrologic export by upscaling the reach-scale estimates of F_{CO_2} to the entire length of the stream. Using total stream bed area estimates (dry season = 3008 m², wet season = 5022 m²; Oviedo-Vargas et al. 2015) and assuming F_{CO_2} in our reach is consistent throughout the entire length of the stream, we estimate total stream mean daily F_{CO_2} of $1499 \pm 1038 \text{ mol CO}_2 \text{ d}^{-1}$. In contrast, we multiply aqueous CO_2 by hourly discharge and estimate a mean daily CO_2 export of $8.2 \pm 10.0 \text{ mol CO}_2 \text{ d}^{-1}$ from Taconazo. This rough comparison shows F_{CO_2} is a 182-times greater fate of CO_2 compared to downstream export and further highlighting the importance of studying F_{CO_2} in tropical streams (Cole et al. 2007; Raymond et al. 2013).

Influence on pH

Small et al. (2012) hypothesized that CO_2 from terrestrial sources enter streams with low solutes and reduce pH through carbonic acid creation, primarily during the early wet season in streams at La Selva. Our results provide some support for this hypothesis.

We show GW_{CO_2} has a negative correlation with stream pH (Fig. 7). In the late dry and early wet season (April–May, Fig. 2), small inputs of GW_{CO_2} can reduce mean daily pH to as low as 4.5. During the wet season (June onward), greater GW_{CO_2} reduce pH to between ~5. Taconazo has low alkalinity (< 10 $\mu\text{eq L}^{-1}$, Ardón et al. 2013), therefore the acid neutralizing capacity is overcome by small inputs of CO_2 . CO_2 is supplemented by increased DOC during storm events (mean stormflow DOC = 2.25 mg L⁻¹, Ganong et al. 2015; Osburn et al. 2018) and redox reactions (e.g., Fe^{2+} oxidation) which can collectively reduce pH. During the wet season, DOC inputs to Taconazo are disproportionately organic acids (Osburn et al. 2018) which have a pK_a that contributes to lower pH. Decreased pH concurrent with higher CO_2 fluxes has been shown in temperate (Aho et al. 2021a) and boreal streams (Wallin et al. 2010), showing the importance of CO_2 fluxes on stream chemistry.

Conclusions

To our knowledge, ours is the first empirical study to investigate relative contributions of internal production and terrestrial sources of CO_2 to tropical streams. We found in-stream metabolism to be a net contributor to the CO_2 pool, with similar estimates of NEP to streams in across the tropics (Marzolf and Ardón 2021). We also found F_{CO_2} to be consistent with previous measurements based on grab samples (Oviedo-Vargas et al. 2015), rather than using sensors, and comparable to headwater streams. Interestingly, internal production of CO_2 as NEP appears to be a more important contributor to F_{CO_2} than were terrestrial inputs, based on estimates of GW_{CO_2} . This finding is somewhat in contrast to models from temperate stream ecosystems (Hotchkiss et al. 2015), and raises questions on the role of sediment and anaerobic respiration in lowland tropical streams, like Taconazo.

In a global synthesis of efflux from inland waters, both Cole et al. (2007) and Raymond et al. (2013) stress the importance of evasion estimates from headwater tropical streams, which exhibit higher reaeration velocities and higher $p\text{CO}_2$. We document sustained high $p\text{CO}_2$ leads to higher F_{CO_2} (Raymond et al. 2013). Our study provides estimates of C fluxes from a stream type with disproportionate influence

among inland waters, contributing to a major knowledge gap in the terrestrial C cycle.

Acknowledgements We are grateful to Minor Hidalgo for help in the field and sensor calibration and maintenance. This study was aided by Laura Willson and the Organization for Tropical Studies Research Experience for Undergraduates program. Dr. Mark Johnson aided in setting up and interpreting CO₂ sensor data. Funding was provided by National Science Foundation DEB award #1655869. We are grateful to members of the Ardón Lab and Dr. Diego Riveros-Iregui for their comments on early drafts of the manuscript. The manuscript was greatly improved following comments from two anonymous reviewers.

Author contributions Conceptualization: NM, CS, DO-V, CG, JD, DG, MA; Methodology: NM, CS, CG, DO-V, DG, MA; Formal analysis and investigation: NM, CS, DO-V, DG, MA; Writing - original draft preparation: NM, CS, MA; Writing - review and editing: all authors; Funding acquisition: MA, AR, CP; Resources: CS, DO-V, DG, CG, MA; Supervision: MA, AR, CP.

Funding Funding was provided by National Science Foundation (NSF) Long-Term Research in Environmental Biology (LTREB) program (award #1655869).

Data availability Data, code, and supplementary material from this study can be accessed at https://github.com/nmarzof91/Taconazo_CO2.

Code availability Data, code, and supplementary material from this study can be accessed at https://github.com/nmarzof91/Taconazo_CO2.

Declarations

Conflict of interest The authors have no relevant financial or non-financial interests to disclose.

Ethical approval Not applicable.

Consent to participate Not applicable.

Consent for publication Not applicable.

References

Aho KS, Fair JH, Hosen JD et al (2021a) Distinct concentration-discharge dynamics in temperate streams and rivers: CO₂ exhibits chemostasis while CH₄ exhibits source limitation due to temperature control. *Limnol Oceanogr* 66:3656–3668. <https://doi.org/10.1002/lio.11906>

Aho KS, Hosen JD, Logozzo LA et al (2021b) Highest rates of gross primary productivity maintained despite CO₂ depletion in a temperate river network. *Limnol Oceanogr Lett* 6:200–206

Appling AP, Hall RO, Yackulic CB, Arroita M (2018) Overcoming Equifinality: Leveraging Long Time Series for Stream Metabolism Estimation. *J Geophys Res Biogeosciences* 123:624–645. <https://doi.org/10.1002/2017JG004140>

Ardón M, Stallcup LA, Pringle CM (2006) Does leaf quality mediate the stimulation of leaf breakdown by phosphorus in Neotropical streams? *Freshw Biol* 51:618–633. <https://doi.org/10.1111/j.1365-2427.2006.01515.x>

Ardón M, Duff JH, Ramírez A et al (2013) Experimental acidification of two biogeochemically-distinct neotropical streams: Buffering mechanisms and macroinvertebrate drift. *Sci Total Environ* 443:267–277. <https://doi.org/10.1016/j.scitotenv.2012.10.068>

Aufdenkampe AK, Mayorga E, Raymond PA et al (2011) Riverine coupling of biogeochemical cycles between land, oceans, and atmosphere. *Front Ecol Environ* 9:53–60. <https://doi.org/10.1890/100014>

Battin TJ, Luysaert S, Kaplan LA et al (2009) The boundless carbon cycle. *Nat Geosci* 2:598–600. <https://doi.org/10.1038/ngeo618>

Solomon DK, Genereux DP, Plummer LN, Busenberg E (2010) Testing mixing models of old and young groundwater in a tropical lowland rain forest with environmental tracers. *Water Resour Res* 46:1–14. <https://doi.org/10.1029/2009WR008341>

Bond N (2021) hydrostats: Hydrologic Indices for Daily Time Series Data

Borges AV, Darchambeau F, Lambert T et al (2019) Variations in dissolved greenhouse gases (CO₂, CH₄, N₂O) in the Congo River network overwhelmingly driven by fluvial-wetland connectivity. *Biogeosciences* 16:3801–3834. <https://doi.org/10.5194/bg-16-3801-2019>

Campeau A, Lapierre JF, Vachon D, Del Giorgio PA (2014) Regional contribution of CO₂ and CH₄ fluxes from the fluvial network in a lowland boreal landscape of Québec. *Global Biogeochem Cycles* 28:57–69. <https://doi.org/10.1002/2013GB004685>

Cole JJ, Prairie YT, Caraco NF et al (2007) Plumbing the global carbon cycle: integrating inland waters into the Terrestrial Carbon Budget. *Ecosystems* 10:172–185. <https://doi.org/10.1007/s10021-006-9013-8>

Colvin SAR, Sullivan SMP, Shirey PD et al (2019) Headwater streams and wetlands are critical for sustaining fish, fisheries, and ecosystem services. *Fisheries* 44:73–91. <https://doi.org/10.1002/fsh.10229>

Crawford JT, Stanley EH, Dornblaser MM, Striegl RG (2017) CO₂ time series patterns in contrasting headwater streams of North America. *Aquat Sci* 79:473–486. <https://doi.org/10.1007/s00027-016-0511-2>

de Rasera MFFL, Krusche AV, Richey JE et al (2013) Spatial and temporal variability of pCO₂ and CO₂ efflux in seven Amazonian Rivers. *Biogeochemistry* 116:241–259. <https://doi.org/10.1007/s10533-013-9854-0>

Demars BOL (2019) Hydrological pulses and burning of dissolved organic carbon by stream respiration. *Limnol Oceanogr* 64:406–421. <https://doi.org/10.1002/lio.11048>

Drake TW, Raymond PA, Spencer RGM (2018) Terrestrial carbon inputs to inland waters: a current synthesis of estimates and uncertainty. *Limnol Oceanogr Lett* 3:132–142. <https://doi.org/10.1002/lio2.10055>

Ganong CN, Small GE, Ardón M et al (2015) Interbasin flow of geothermally modified ground water stabilizes stream exports of biologically important solutes against variation in precipitation. *Freshw Sci* 34:276–286. <https://doi.org/10.1086/679739>

Ganong C, Hidalgo Oconitrillo M, Pringle C (2021) Thresholds of acidification impacts on macroinvertebrates adapted to seasonally acidified tropical streams: potential responses to extreme drought-driven pH declines. *PeerJ* 9:e11955. <https://doi.org/10.7717/peerj.11955>

Genereux DP, Jordan M (2006) Interbasin groundwater flow and groundwater interaction with surface water in a lowland rainforest, Costa Rica: a review. *J Hydrol* 320:385–399. <https://doi.org/10.1016/j.jhydrol.2005.07.023>

Genereux DP, Jordan MT, Carbonell D (2005) A paired-watershed budget study to quantify interbasin groundwater flow in a lowland rain forest. Costa Rica. *Water Resour Res* 41:10. <https://doi.org/10.1029/2004WR003635>

Genereux DP, Webb M, Solomon DK (2009) Chemical and isotopic signature of old groundwater and magmatic solutes in a Costa Rican rain forest: Evidence from carbon, helium, and chlorine. *Water Resour Res* 45:1–14. <https://doi.org/10.1029/2008WR007630>

Genereux DP, Nagy LA, Osburn CL, Oberbauer SF (2013) A connection to deep groundwater alters ecosystem carbon fluxes and budgets: Example from a Costa Rican rainforest. *Geophys Res Lett* 40:2066–2070. <https://doi.org/10.1002/grl.50423>

Stoddard JL, Jeffries DS, Lükewille A et al (1999) Regional trends in aquatic recovery from acidification in North America and Europe. *Nature* 401:575–578

Gómez-Gener L, Rocher-Ros G, Battin T et al (2021) Global carbon dioxide efflux from rivers enhanced by high nocturnal emissions. *Nat Geosci* 14:289–294. <https://doi.org/10.1038/s41561-021-00722-3>

Stumm W, Morgan JJ (1996) Dissolved Carbon Dioxide. In: *Aquatic chemistry: chemical equilibria and rates in natural waters*, 3rd editio. Wiley, New York

Hall RO, Hotchkiss ER (2017) Stream Metabolism. In: Lamberti GA, Hauer FR (eds) *Methods in Stream Ecology*, Vol 2: Ecosystem Function, 3rd Edition. Academic Press Ltd-Elsevier Science Ltd, pp 219–233

Hall RO, Ulseth AJ (2020) Gas exchange in streams and rivers. *WIREs Water* 7:e1391. <https://doi.org/10.1002/wat2.1391>

Hurley A (2021) datacleanr: Interactive and Reproducible Data Cleaning

Haque MM, Begum MS, Nayna OK et al (2022) Seasonal shifts in diurnal variations of pCO₂ and O₂ in the lower Ganges River. *Limnol Oceanogr Lett* 7:191–201. <https://doi.org/10.1002/lo2.10246>

Tank SE, Fellman JB, Hood E, Kritzberg ES (2018) Beyond respiration: controls on lateral carbon fluxes across the terrestrial-aquatic interface. *Limnol Oceanogr Lett* 3:76–88. <https://doi.org/10.1002/lo2.10065>

Hotchkiss ER, Hall RO Jr, Sponseller RA et al (2015) Sources of and processes controlling CO₂ emissions change with the size of streams and rivers. *Nat Geosci* 8:696–699. <https://doi.org/10.1038/ngeo2507>

Johnson MS, Lehmann J, Riha SJ et al (2008) CO₂ efflux from Amazonian headwater streams represents a significant fate for deep soil respiration. *Geophys Res Lett* 35:L17401. <https://doi.org/10.1029/2008gl034619>

Johnson MS, Billell MF, Dinsmore KJ et al (2010) Direct and continuous measurement of dissolved carbon dioxide in freshwater aquatic systems-method and applications. *Ecohydrology*. <https://doi.org/10.1002/eco.95>

Kay M, Wobbrock J (2020) ARTTool: aligned rank transform for nonparametric factorial ANOVAs

Ladson A, Brown R, Neal B, Nathan R (2013) A standard approach to baseflow separation using the Lyne and Hollick filter. *Aust J Water Resour* 17:25–34. <https://doi.org/10.7158/W12-028.2013.17.1>

Liu S, Kuhn C, Amatulli G et al (2022) The importance of hydrology in routing terrestrial carbon to the atmosphere via global streams and rivers. *Proc Natl Acad Sci*. <https://doi.org/10.1073/pnas.2106322119>

Lupon A, Denfeld BA, Laudon H et al (2019) Groundwater inflows control patterns and sources of greenhouse gas emissions from streams. *Limnol Oceanogr* 64:1545–1557. <https://doi.org/10.1002/lno.11134>

Marzolf NS, Ardón M (2021) Ecosystem metabolism in tropical streams and rivers: a review and synthesis. *Limnol Oceanogr* 66:1627–1638. <https://doi.org/10.1002/lno.11707>

Wetzel RG, Likens GE (2000) The inorganic carbon complex: alkalinity, acidity, CO₂, pH, total inorganic carbon, hardness, aluminum. In: *Limnological analyses*. Springer, pp 113–135

Mayorga E, Aufdenkampe AK, Masiello CA et al (2005) Young organic matter as a source of carbon dioxide outgassing from Amazonian rivers. *Nature* 436:538–541. <https://doi.org/10.1038/nature03880>

Osburn CL, Oviedo-Vargas D, Barnett E et al (2018) Regional groundwater and storms are hydrologic controls on the quality and export of dissolved organic matter in two tropical Rainforest Streams, Costa Rica. *J Geophys Res Biogeosci* 123:850–866. <https://doi.org/10.1002/2017JG003960>

Oviedo-Vargas D, Genereux DP, Dierick D, Oberbauer SF (2015) The effect of regional groundwater on carbon dioxide and methane emissions from a lowland rainforest stream in Costa Rica. *J Geophys Res Biogeosci* 120:2579–2595. <https://doi.org/10.1002/2015JG003009>

Plummer LN, Busenberg E (1982) The solubilities of calcite, aragonite and vaterite in CO₂-H₂O solutions between 0 and 90°C, and an evaluation of the aqueous model for the system CaCO₃-CO₂-H₂O. *Geochim Cosmochim Acta* 46:1011–1040. [https://doi.org/10.1016/0016-7037\(82\)90056-4](https://doi.org/10.1016/0016-7037(82)90056-4)

R Core Team (2022) R: a language and environment for statistical computing

Ramírez A, Pringle CM, Molina L (2003) Effects of stream phosphorus levels on microbial respiration. *Freshw Biol* 48:88–97. <https://doi.org/10.1046/j.1365-2427.2003.00973.x>

Raymond PA, Zappa CJ, Butman D et al (2012) Scaling the gas transfer velocity and hydraulic geometry in streams and small rivers. *Limnol Oceanogr Fluids Environ* 2:41–53. <https://doi.org/10.1215/21573689-1597669>

Taylor JR, Loescher HL (2013) Automated quality control methods for sensor data: a novel observatory approach.

Biogeosciences 10:4957–4971. <https://doi.org/10.5194/bg-10-4957-2013>

Raymond PA, Hartmann J, Lauerwald R et al (2013) Global carbon dioxide emissions from inland waters. *Nature* 503:355–359. <https://doi.org/10.1038/nature12760>

Richey JE, Melack JM, Aufdenkampe AK et al (2002) Outgassing from Amazonian rivers and wetlands as a large tropical source of atmospheric CO₂. *Nature* 416:617–620. <https://doi.org/10.1038/416617a>

Rocher-Ros G, Sponseller RA, Bergström A et al (2020) Stream metabolism controls diel patterns and evasion of CO₂ in Arctic streams. *Glob Chang Biol* 26:1400–1413. <https://doi.org/10.1111/gcb.14895>

Rocher-Ros G, Harms TK, Sponseller RA et al (2021) Metabolism overrides photo-oxidation in CO₂ dynamics of Arctic permafrost streams. *Limnol Oceanogr* 66:S169–S181. <https://doi.org/10.1002/lo.11564>

Vachon D, Sadro S, Bogard MJ et al (2020) Paired O₂–CO₂ measurements provide emergent insights into aquatic ecosystem function. *Limnol Oceanogr Lett* 5:287–294. <https://doi.org/10.1002/lo2.10135>

Rosemond AD, Pringle CM, Ramírez A et al (2002) Landscape variation in phosphorus concentration and effects on detritus-based tropical streams. *Limnol Oceanogr* 47:278–289. <https://doi.org/10.4319/lo.2002.47.1.00278>

Sanford RL, Paaby P, Luvall JC, Phillips E (1994) Climate, geomorphology, and aquatic systems. In: McDade LA, Bawa KS, Hespenheide HA, Hartshorn GS (eds) *La Selva: Ecology and natural history of a Neotropical rain forest*. University of Chicago Press, pp 19–33

Schneider CL, Herrera M, Raisle ML et al (2020) Carbon dioxide (CO₂) fluxes from terrestrial and aquatic environments in a high-altitude tropical catchment. *J Geophys Res Biogeosci* 125. <https://doi.org/10.1029/2020JG005844>

Small GE, Ardón M, Jackman AP et al (2012) Rainfall-driven amplification of seasonal acidification in poorly buffered tropical streams. *Ecosystems* 15:974–985. <https://doi.org/10.1007/s10021-012-9559-6>

Wallin M, Buffam I, Öquist M et al (2010) Temporal and spatial variability of dissolved inorganic carbon in a boreal stream network: concentrations and downstream fluxes. *J Geophys Res Biogeosci*. <https://doi.org/10.1029/2009JG001100>

Zanon C, Genereux DP, Oberbauer SF (2014) Use of a watershed hydrologic model to estimate interbasin groundwater flow in a Costa Rican rainforest. *Hydrol Process* 28:3670–3680. <https://doi.org/10.1002/hyp.9917>

Publisher's Note Springer Nature remains neutral with regard to jurisdictional claims in published maps and institutional affiliations.